

# Con ned Water: Comparison between a Purely Repulsive Con nem ent and Hydrophobic Lennard-Jones Con nem ent

Pradeep Kumar,<sup>1</sup> Francis W . Starr,<sup>2</sup> Sergey V . Buldyrev,<sup>3</sup> and H . Eugene Stanley<sup>1</sup>

<sup>1</sup>Center for Polymer Studies and Department of Physics

Boston University, 590 Commonwealth Avenue, Boston, MA 02215 USA

<sup>2</sup>Department of Physics, Wesleyan University, Middletown, CT 06459 USA

<sup>3</sup>Department of Physics, Yeshiva University,

500 West 185th Street, New York, NY 10033 USA

(Dated: last revised: 30 March 2006, ksbs.tex)

## Abstract

M uch of the understanding of bulk liquids has progressed through study of the limiting case in which molecules interact via purely repulsive forces, such as a hard-core potential. In the same spirit, we report progress on the understanding of con ned water by examining the behavior of water-like molecules interacting with walls via purely repulsive forces. Specifically, we perform molecular dynamics simulations of 512 water-like molecules which are con ned between two smooth plates that are separated by 1.1 nm and are interacting via the TIP5P potential. At this separation, there are either two or three molecular layers of water, depending on density. We systematically compare our results with purely repulsive interactions between molecules and the walls with those obtained for Lennard-Jones (LJ) interactions between the molecules and the walls. We nd that the thermodynamic, dynamical and structural properties of the liquid qualitatively match those for a system with a LJ attraction to the wall. In previous studies that include attractions, freezing into monolayer or trilayer ice was seen for this wall separation. Using the same separation as these previous studies, we nd that the crystal state is not stable with repulsive walls. However, by carefully adjusting the separation of the plates with repulsive interactions so that the effective space available to the molecules is the same as that for LJ con nem ent, we nd that the same crystal phases are stable. This result emphasizes the importance of comparing systems only using the same effective con nem ent, which may differ from the geometric separation of the con ning surfaces.

## I. INTRODUCTION

Confinement of water in nanopores affects many properties of water, such as freezing temperature, crystal structure [1, 2, 3, 9, 18], the glass transition temperature, and the position of the hypothesized liquid-liquid (LL) critical point [4, 5, 6, 7, 8]. Indeed, water confined in nanoscale has received much recent attention, in part because of its importance in biology, engineering, geophysics and atmospheric sciences. The effects of different kinds of confinement have been studied, both using experiments and simulations [2, 9, 10, 11, 12, 13, 14].

Supercooled water (bulk water cooled below the equilibrium freezing temperature) shows many anomalous properties [15, 16, 17, 18]. Experiments find that at low temperatures, various response functions, such as isothermal compressibility and specific heat, increase sharply. This unusual behavior is explainable by the presence of a LL phase transition line separating two liquid states of different densities and terminating at a LL critical point [19, 20, 21, 22, 23, 24, 25, 26, 27, 28, 29, 30, 31]. There has been comparatively less research on confined water. Using the ST2 potential to model water confined between smooth plates [32], a LL phase transition has been proposed. A liquid-to-amorphous transition is seen in simulations of water using the TIP4P potential [33] confined in carbon nanotubes [2]. Recent theoretical work [34] suggests that hydrophobic Lennard-Jones (LJ) confinement shifts the LL transition to lower temperature and lower pressure compared to bulk water, a feature also found in simulations of water confined between hydrophobic plates [12].

Recent work has also focused on understanding the effects of confinement on the glass transition, which is related to the structural relaxation of molecules at low temperature. As temperature is lowered, a characteristic correlation length  $\xi$ , the length scale at which the structural rearrangement should occur in order for system to relax, grows [35, 36, 37]. In confinement cannot grow indefinitely because of the finite size, and thus it is interesting to understand how confinement affects the glass transition temperature  $T_g$ . Simulations of supercooled bulk water using the SPC/E potential show that the dynamics at low temperature agree with the predictions of mode coupling theory (MCT) [38, 39, 40]. Confinement is also expected to shift  $T_g$ , as studied extensively in polymeric systems [41]. As the effects of confinement are reduced by increasing the distance between the two walls,  $T_g$  approaches that of the bulk system [41]. In experiments on bulk water,  $T_g$  is difficult to obtain, since

water freezes spontaneously at low temperatures. Therefore a good understanding of confined geometries, where freezing might be avoided down to very low temperatures, might help elucidate the nature of glass transition in water.

Confined water is known to enhance solidification of molecules that are more or less spherical [42, 43, 44]. However, careful experiments on thin films of water show that water performs extremely well as a lubricant, suggesting that confined water may be more fluid than bulk water [45]. Recent experiments show that water in hydrophilic confinement, when cooled to very low  $T$ , does not freeze [6] (a phenomenon also supported by simulation studies [46, 47]). In contrast, simulations [2, 9, 10, 11, 12, 13] show that hydrophobically confined water does freeze into different crystalline structures, which do not have counterparts in bulk water. Monolayer, bilayer and trilayer ice have all been found in simulations [2, 9, 10, 11, 12, 13]. Indeed hydrophobic confinement seems to facilitate the freezing of water.

In this work, we study the effect of confinement on thermodynamics, structure, and the freezing of water in case when the water-wall interactions are purely repulsive ("repulsive confinement"). We also compare the freezing in repulsive confinement with the freezing found when the water-wall interactions are represented by an LJ interaction ("LJ hydrophobic confinement") [9, 12].

This paper is organized as follows: In Sec. II, we provide details of our simulations and analysis methods. Simulation results for the liquid state are provided in Sec. III. In Sec. IV we discuss the freezing properties of our system, followed by a brief conclusion.

## II. SIMULATION AND ANALYSIS METHODS

We perform molecular dynamics (MD) simulations of a system composed of water-like molecules confined between two smooth walls. The molecules interact via the TIP5P pair potential [48] which, like the ST2 [49] potential, treats each water molecule as a tetrahedral, rigid, and non-polarizable unit consisting of five point sites. Two positive point charges of charge  $q_H = 0.241e$  (where  $e$  is the fundamental unit of charge) are located on each hydrogen atom at a distance 0.09572 nm from the oxygen atom; together they form an H O H angle of 104.52°. Two negative point charges ( $q_O = -q_H$ ) representing the lone pair of electrons ( $e^-$ ) are located at a distance 0.07 nm from the oxygen atom. These negative point charges are located in a plane perpendicular to the H O H plane and form an e O e

angle of  $\cos^{-1}(1/3) = 109.47^\circ$ , the tetrahedral angle. To prevent overlap of molecules, a fifth interaction site is located on the oxygen atom, and is represented by a LJ potential with parameters  $\sigma_{oo} = 0.312$  nm and  $\epsilon_{oo} = 0.6694$  kJ/mol.

The TIP5P potential predicts many of the anomalies of bulk water [50]. For example, TIP5P reproduces the density anomaly at  $T = 277$  K and  $P = 1$  atm and its structural properties compare well with experiments [48, 50, 51, 52, 53]. TIP5P is known to crystallize at high pressures [50] within accessible computer simulation time scales, and shows a "nose-shaped" curve of temperature versus crystallization time [50], a feature found in experimental data on water solutions [54].

In our simulations,  $N = 512$  water molecules are confined between two infinite smooth planar walls, as shown schematically in Fig. 1. The walls are located at  $z_w = 0.55$  nm (wall-wall separation of 1.1 nm), which results in 2–3 layers of water molecules. Periodic boundary conditions are used in the x and y directions, parallel to the walls.

The interaction between water molecules and the smooth walls is given by

$$U(z) = 4 \epsilon_{ow} \left( \frac{r_{ow}}{z - z_w} \right)^2 + \frac{1}{2} \epsilon_{ow}^3 \left( \frac{r_{ow}}{z - z_w} \right)^5 \quad (1)$$

Here  $|z - z_w|$  is the distance from the oxygen atom of a water molecule to the wall, while  $\epsilon_{ow} = 1.0$  kJ/mole and  $r_{ow} = 0.25$  nm are potential parameters (Fig. 2). The same parameter values were used in previous confined water simulations using the TIP5P interaction potential [12].

We perform simulations for 56 state points, corresponding to seven temperatures  $T = 220$ , 230, 240, 250, 260, 280, and 300 K, and eight raw "geometric" densities  $\rho = 0.60, 0.655, 0.709, 0.764, 0.818, 0.873, 0.927$  and  $0.981$  g/cm<sup>3</sup> (the same as those studied in ref. [12]). The geometric values of density do not take into account the fact that the repulsive interactions of molecules with the walls increases the overall amount of available space. For systems confined by LJ interactions, there is a well-defined preferred distance from the wall, making it relatively straightforward to evaluate the "effective" density of molecules confined by the attractive wall. In our system with only repulsive interactions, there is no such preferred distance, as emphasized by Fig. 2.

We can approximate the effective density for our system by examining the local density  $\rho(z)$  (Fig. 3). We utilize that fact that  $\rho(z)$  has an inflection, and estimate the effective  $L_z$  by the location where the second derivative of  $\rho(z) = 0$ , or when the first derivative of  $\rho(z)$

has a maximum. We must also add to this value the molecular diameter of water (0.278 nm) to calculate the real space available along z-direction. The resulting effective densities are = 0.715, 0.777, 0.829, 0.890, 0.949, 1.000, 1.060, and 1.115 g/cm<sup>3</sup>. We will use these effective densities throughout the paper, since they will be most comparable to the effective densities with LJ component.

We control the temperature using the Berendsen thermostat with a time constant of 5 ps [55] and use a simulation time step of 1 fs, just as in the bulk system [50]. For all interactions we use a cutoff of 0.9 nm [48].

### III. THERMODYNAMICS AND STRUCTURE

One of the defining characteristics of water is the existence of a temperature of maximum density (TMD). Ref. [12] found that { relative to bulk water { LJ component shifts the locus of TMD the lower T by ~40 K. Additionally, the sharpness of the density maximum is markedly decreased in comparison to the bulk. Fig. 4 shows isochores of P for both LJ component as well as for purely repulsive component for similar densities; a TMD in this plot is coincident with the minimum in the isochore. For repulsive component, the minimum is very weak, but the location of the flatness in the isochore is near to that of the system with LJ component. This result suggests the repulsive component further suppresses the structural ordering of the molecules that is known to be responsible to the presence of a density maximum.

In order to compare the structural properties of repulsive component with those of LJ component, we calculate the lateral oxygen-oxygen radial distribution function (RDF) defined by

$$g_{xy}(r) = \frac{1}{2V} \sum_{i \neq j} \int_{-\infty}^{\infty} \delta(r - r_{ij}) H(z_i - z_j) H(z_i + z_j - z) : \quad (2)$$

Here V is the volume,  $r_{ij}$  is the distance parallel to the walls between molecules i and j,  $z_i$  is the z-coordinate of the oxygen atom of molecule i, and  $\delta(x)$  is the Dirac delta function. The Heaviside functions,  $H(x)$ , restrict the sum to a pair of oxygen atoms of molecules located in the same slab of thickness  $z = 0.1$  nm. The physical interpretation of  $g_{xy}(r)$  is that  $g_{xy}(r)2 \pi r dr dz$  is proportional to the probability of finding an oxygen atom in a slab of thickness  $z$  at a distance  $r$  parallel to the walls from a randomly chosen oxygen atom. In

a bulk liquid, this would be identical to  $g(r)$ , the standard RDF.

Figure 5 shows the temperature and density dependence of the lateral oxygen-oxygen pair correlation function. At low temperature and low density, the first two peaks in  $g_{xy}$  appear at  $r = 2.78 \text{ \AA}$  and  $r = 4.5 \text{ \AA}$ , but at high densities the second peak moves to a larger distance. This behavior is nearly identical to that observed for water confined between LJ surfaces, and is discussed in detail in ref. [12].

We also confirm the structural similarity to ref. [12] by calculating the lateral static structure factor  $S_{xy}(q)$ , defined as the Fourier transform of the lateral radial distribution function  $g_{xy}(r)$ ,

$$S_{xy}(q) = \frac{1}{N} \sum_{i,j}^D e^{iq \cdot (r_i - r_j)} : \quad (3)$$

Here the  $q$ -vector is the inverse space vector in the  $xy$  plane and  $r$  is the projection of the position vector on the  $xy$  plane. In Fig. 6, we show the lateral structure factors for repulsive confinement for different temperatures and densities. We find that confined water has a weaker pre-peak at  $18 \text{ nm}^{-1}$  compared to bulk water (Fig. 7), consistent with the possibility that the local tetrahedrality is weakened by repulsive confinement. Further, we find that the lateral structure of the water in purely repulsive confinement is similar to the lateral structure of LJ-confined water (Fig. 7).

#### IV. FREEZING OF TIP5P WATER

Bulk TIP5P water crystallizes within the simulation time for  $> 1.15 \text{ g/cm}^3$  at low temperatures. For density  $1.20 \text{ g/cm}^3$ , the crystallization time has a minimum at  $T = 240 \text{ K}$  [50]. Crystallization of confined water is seen in some simulations [9, 10, 12]. A similar crystallization appears in simulations when an electric field is applied to a system of water confined between silica walls, in a lateral direction [11].

At plate separation of  $1.1 \text{ nm}$  with hydrophobic LJ confinement, water crystallizes to trilayer ice [12]. From our simulations of TIP5P water in repulsive confinement with the same plate separation of  $1.1 \text{ nm}$ , we find that the system does not freeze within accessible simulation time scales. As a more stringent confirmation of this fact, we also use a starting ice configuration obtained from simulations with LJ confinement for the same thickness, and confirm that the ice melts to a liquid. For a comparison of these two cases, we show in Fig. 8 the evolution of the potential energy of the system with time at  $T = 260 \text{ K}$ . In the

case of LJ confinement, the onset of the crystallization is indicated by a drop in potential energy. In Fig. 9, we show the evolution of potential energy and lateral structure factor with time, when the crystal formed in LJ-confinement [12] is kept between the purely repulsive walls. The potential energy first increases and then reaches its equilibrium value of the liquid potential energy accompanied by a structural changes from a crystal (presence of sharp Bragg peaks) to a liquid (absence of Bragg peaks).

Based on this observation, it is tempting to claim that repulsion inhibits the crystallization, and that a preferable distance from the wall determined by the attractive portion of the LJ potential is necessary to induce crystallization. However, as discussed earlier in the manuscript, for the same plate separation, repulsive confinement increases the available space for molecules relative to LJ confinement. Hence to properly compare the crystallization behavior, it is imperative to adjust the separation of the walls so that the available space for the water molecules is the same in both systems. We can make the available space the same by slightly adjusting the separation of the plates or by tuning the potential in each system. By tuning the parameters (see Fig. 10) of the repulsive potential in the repulsive system such that the density profile along z-axis becomes similar, we have identical values of the available space between the plates (see Fig. 11), and we find that an initial crystal configuration does not melt, emphasizing that the presence of the crystal is very sensitive to density and to plate separation (since the separation determines the accessible packing arrangements between the plates. Similar sensitivity to plate separation for monolayer ice was seen in ref. [11].

In addition to examining the stability of initially crystalline structures, we also consider whether freezing from the liquid state occurs when we have the same effective separation. We find that for the repulsively confined system, the crystal will also spontaneously form if the available space between the plates is the same that where initially crystalline configurations are stable. Hence plate separation appears to be the dominant effect in determining whether or not a crystal will form.

In conclusion, we have investigated the effect of purely repulsive water-wall interactions (repulsive confinement) on freezing of water between two parallel smooth plates. We compare our results with water in hydrophobic LJ confinement, and find that thermodynamic, dynamical and structural properties are qualitatively similar in both cases, but that freezing of water in repulsive confinement is suppressed compared to the freezing in LJ hydrophobic

co n n em ent.

## V . A C K N O W L E D G M E N T S

We thank N . G iovambattista, M . M azza, F . Sciortino, L . Xu and Z . Yan for helpful discussions, and the N SF for support under grants C H E 0096892, C H E 0404699, and D M R - 0427239. We also thank the Boston University computational facility for computational time and the O ce of Academic Affairs at Yeshiva University for support.

---

- [1] R . Zangi, *J. Phys. Cond. M at.* 16, S5371 (2004).
- [2] K . K oga, H . Tanaka, and X . C . Zeng, *Nature* 408, 564 (2000).
- [3] K . K oga and H . Tanaka, *J. Chem . Phys.* 122, 104711 (2005).
- [4] J.-M . Zanotti, M .-C . Bellissent-Funel, and S.-H . Chen, *Phys. Rev. E* 59, 3084 (1999).
- [5] L . Liu, S.-H . Chen, A . Faraone, C .-W . Yen, and C .-Y . Mou, *Phys. Rev. Lett.* 95, 117802 (2005).
- [6] M .-C . Bellissent-Funel, R . Sridhar, and L . Bosio, *J. Chem . Phys.* 104, 10023 (1996).
- [7] L . Xu, P . K um ar, S .V . Buldyrev, S.-H . Chen, P . Poole, F . Sciortino, and H . E . Stanley, *Proc. Nat. Acad. Sci.* 102, 16558 (2005).
- [8] P . K um ar, L . Xu, Z . Yan, M . M azza, S .V . Buldyrev, S.-H . Chen, S . Sastry, and H . E . Stanley (submitt ed).
- [9] K . K oga, X . C . Zeng, and H . Tanaka, *Phys. Rev. Lett.* 79, 5262 (1997).
- [10] R . Zangi and A . E . M ark, *Phys. Rev. Lett.* 91, 0255502 (2003).
- [11] R . Zangi and A . E . M ark, *J. Chem . Phys.* 119, 1694 (2003); *ibid*, 120, 7123 (2004).
- [12] P . K um ar, S .V . Buldyrev, F .W . Starr, N . G iovambattista, and H . E . Stanley, *Phys. Rev. E* 72, 051503 (2005).
- [13] N . G iovambattista, P . Rossky, P . G . D ebenedetti, *Phys. Rev. E* . (in press), (2006).
- [14] J .M arti, G . N agy, M . C . G ordillo, E . G uardia, *J. Chem . Phys.* 124, 094703 (2006).
- [15] P . G . D ebenedetti, *J. Phys. Cond. M at.* 15, R 1669 (2003).
- [16] P . G . D ebenedetti and H . E . Stanley, *Physics Today* 56 (6), 40 (2003).
- [17] C .A . A ngell, *Ann. Rev. Phys. Chem.* 55, 559 (2004).

[18] M .C . Bellissent Funnel, ed., *Hydration Processes in Biology: Theoretical and Experimental Approaches* [NATO ASI Series A, Vol. 305] (IOS Press, Amsterdam, 1998).

[19] P .H . Poole, F . Sciortino, U . E ssman, and H .E . Stanley, *Nature* 360, 324 (1992).

[20] O .M ishim a and H .E . Stanley, *Nature* 396, 329 (1998); *ibid* 392 164 (1998).

[21] P .H . Poole, F . Sciortino, T . G rande, H .E . Stanley, and C .A . Angell, *Phys. Rev. Lett.* 73, 1632 (1994).

[22] F . Sciortino, P .H . Poole, U . E ssman, and H .E . Stanley, *Phys. Rev. E* 55, 727 (1997).

[23] H .E . Stanley, L .C ruiz, S .T . Harrington, P .H . Poole, S .Sastry, F . Sciortino, F .W . Starr, and R .Zhang, *Physica A* 236, 19 (1997).

[24] F . Sciortino, E . La N ave, and P .Tartaglia, *Phys. Rev. Lett.* 91, 155701 (2003).

[25] G .Franzese, M . I.M argues, and H .E . Stanley, *Phys. Rev. E* 67, 011103 (2003).

[26] V .B razhkin, S .V . Buldyrev, V .N .R yzhov, and H .E . Stanley, eds., *New K inds of Phase Transitions: Transform ations in D isordered Substances* (Kluwer, Dordrecht, 2002).

[27] D .Paschek, *Phys. Rev. Lett.* 94, 217802 (2005).

[28] P .K um ar, S .V . Buldyrev, F . Sciortino, E .Zaccarelli, and H .E . Stanley, *Phys. Rev. E* 72, 021501 (2005).

[29] L .X u, P .K um ar, S .V . Buldyrev, S .H .C hen, P .H . Poole, F . Sciortino, and H .E . Stanley, *Proc. of Nat. Acad. Sci.* 102, 16558 (2005).

[30] G .Franzese, G .M alecio, A .Skibinsky, S .V . Buldyrev and H .E . Stanley, *Nature* 409, 692 (2001).

[31] S .H arrington, P .H . Poole, F . Sciortino, and H .E . Stanley, *J. Chem .Phys.* 107, 7443 (1997).

[32] M .M eyer and H .E . Stanley, *J. Phys. Chem .B* 103, 9728 (1999).

[33] W .L .Jorgensen, J .Chandrasekhar, J .M adura, R .W .Impey and M .K lein, *J. Chem .Phys.* 79, 926 (1983).

[34] T .M .Truskett, P .G .D ebenedetti, and S .Torquato, *J. Chem .Phys.* 114, 2401 (2001).

[35] N .L aćević, et al., *J. Chem .Phys.* 119, 7372 (2003); *Phys. Rev. E* 66, 030101 (2002).

[36] L .Berthier, G .B iroli, J .P .Bouchaud, L .C ipelletti, D .E lMasri, D .L 'H te, F .L adieu, M .P iemo, *Science* 310, 1797 (2005).

[37] P .Scheidler, W .K ob, and K .B inder, *Europhys. Lett.* 59, 701 (2002).

[38] W .G otze, in *Liquids, Freezing and the Glass Transition*, *Proceedings of the Les Houches Summer School of Theoretical Physics*, Session LI, 1989, edited by J .P .Hansen, D .Levesque,

and J. Zinn-Justin (North-Holland, Amsterdam, 1991).

- [39] P. Gallo, F. Sciortino, P. Tartaglia, and S.-H. Chen, *Phys. Rev. Lett.* **76**, 2730 (1996).
- [40] P. Kumar, G. Franzese, S.V. Buldyrev, and H.E. Stanley, *Phys. Rev. E* (in press).
- [41] J. Baschnagel and F. Vamik, *J. Phys.: Cond. Matt.* **17** (2005) R 851.
- [42] C. Rhykerd, M. Schoen, D. Duester, and J. Cushman, *Nature* (London) **330**, 461 (1989); P. A. Thompson and M.O. Robbins, *Science* **250**, 792 (1990).
- [43] B. Brushan, J.N. Israelachvili, and U. Landman, *Nature* (London) **374**, 607 (1995).
- [44] B.N.J. Persson, *Sliding Friction: Physical Principles and Applications*, Springer, Heidelberg, 1998.
- [45] A.M. Homola, J.N. Israelachvili, M.L. Gee, and P.M.M. Guiggan, *J. Tribology* **111**, 675 (1989); J.N. Israelachvili, *Surf. Sci. Rep.* **14**, 109 (1992).
- [46] P. Gallo, M. Rovere and E. Spohr, *J. Chem. Phys.* **113**, 11324 (2000).
- [47] P. Gallo, *Phys. Chem. Chem. Phys.* **2**, 1607 (2000).
- [48] M.W. Mahoney and W.L. Jorgensen, *J. Chem. Phys.* **112**, 8190 (2000).
- [49] F.H. Stillinger and A. Rahman, *J. Chem. Phys.* **60**, 1545 (1974).
- [50] M. Yamada, S. Mossa, H.E. Stanley, and F. Sciortino, *Phys. Rev. Lett.* **88**, 195701 (2002).
- [51] M.W. Mahoney and W.L. Jorgensen, *J. Chem. Phys.* **114**, 363 (2001).
- [52] J.M. Sorenson, G. Hura, R.M. Glaeser, and T. Head-Gordon, *J. Chem. Phys.* **113**, 9149 (2000).
- [53] P. Kumar, S.V. Buldyrev, and H.E. Stanley, *Proc. NATO ASW*, Odessa, Ed. V. Mazur (Springer, Heidelberg, 2006).
- [54] L.A. Baez and P. Clancy, *J. Chem. Phys.* **103**, 9744 (1995).
- [55] H.J.C. Berendsen, J.P.M. Postma, W.F. van Gunsteren, A.D. Nola and J.R. Haak, *J. Chem. Phys.* **81**, 3684 (1984).

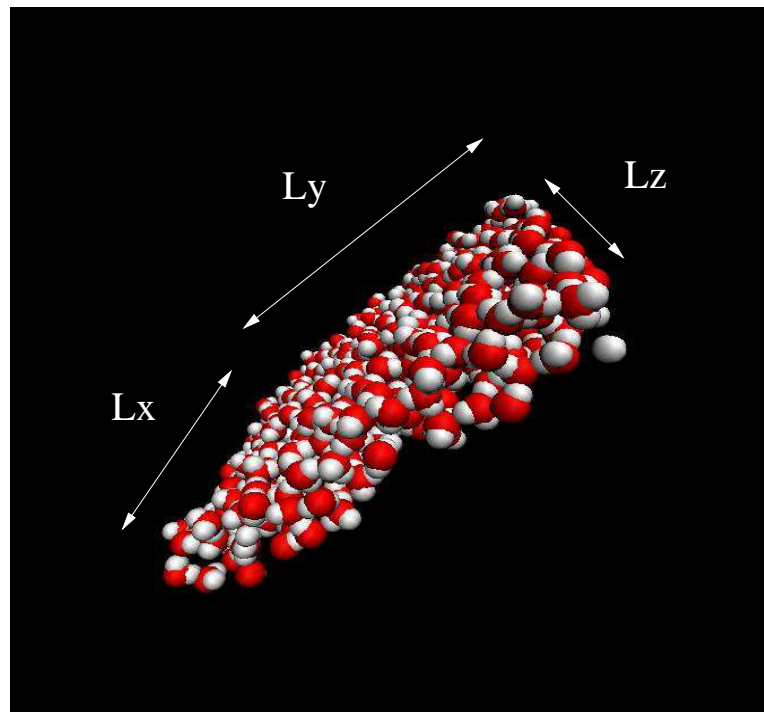


FIG . 1: Perspective view of the system , showing the 512 water molecules confined between two walls perpendicular to the z-direction .

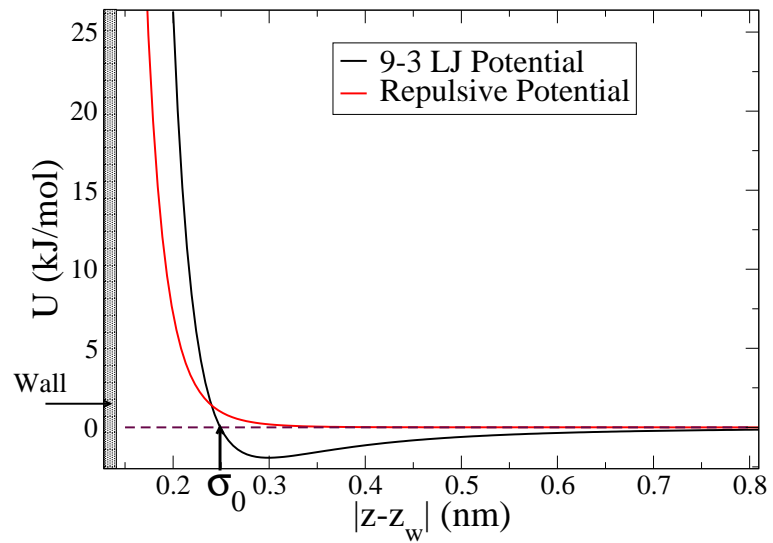


FIG . 2: Water-wall interaction potential as a function of distance of water molecules  $|z - z_w|$  from the center of one of the walls (shaded rectangle).

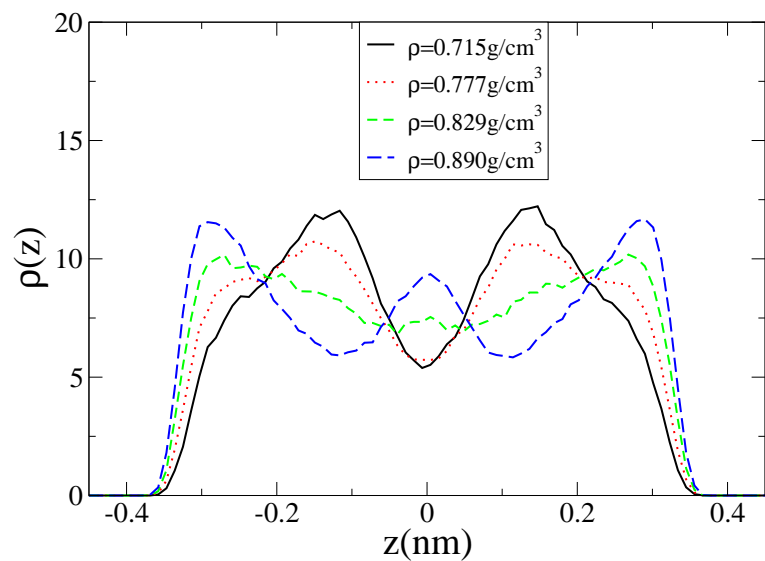


FIG . 3: Density profile ( $\rho_z$ ) along  $z$ -direction for four different bulk densities at  $T = 250$  K .

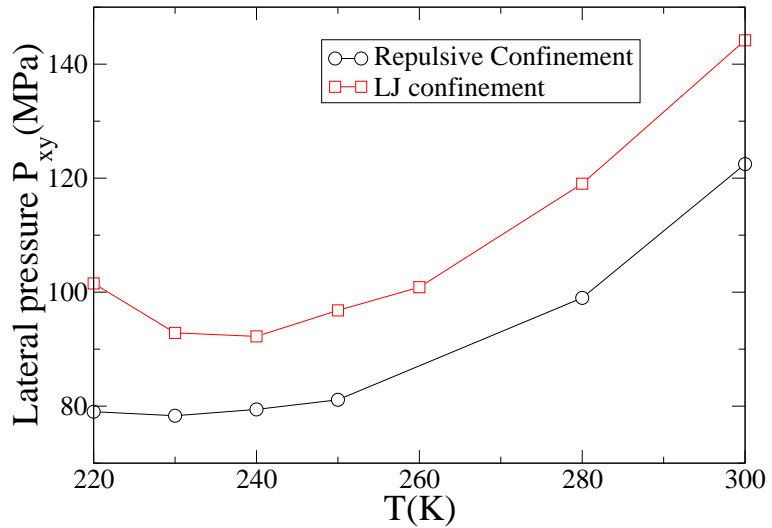


FIG .4: Lateral pressure  $P_{xy}$  for one isochore for both the purely repulsive and LJ confinement cases. Here the effective density is  $= 0.829 \text{ g/cm}^3$  for the purely repulsive potential and  $= 0.950 \text{ g/cm}^3$  for LJ confinement. These effective densities for both systems correspond to the same "raw" geometric density of  $0.709 \text{ g/cm}^3$ . Both forms of confinement show a TMD, indicated by the minimum of the pressure; however the TMD is very flat for repulsive confinement.

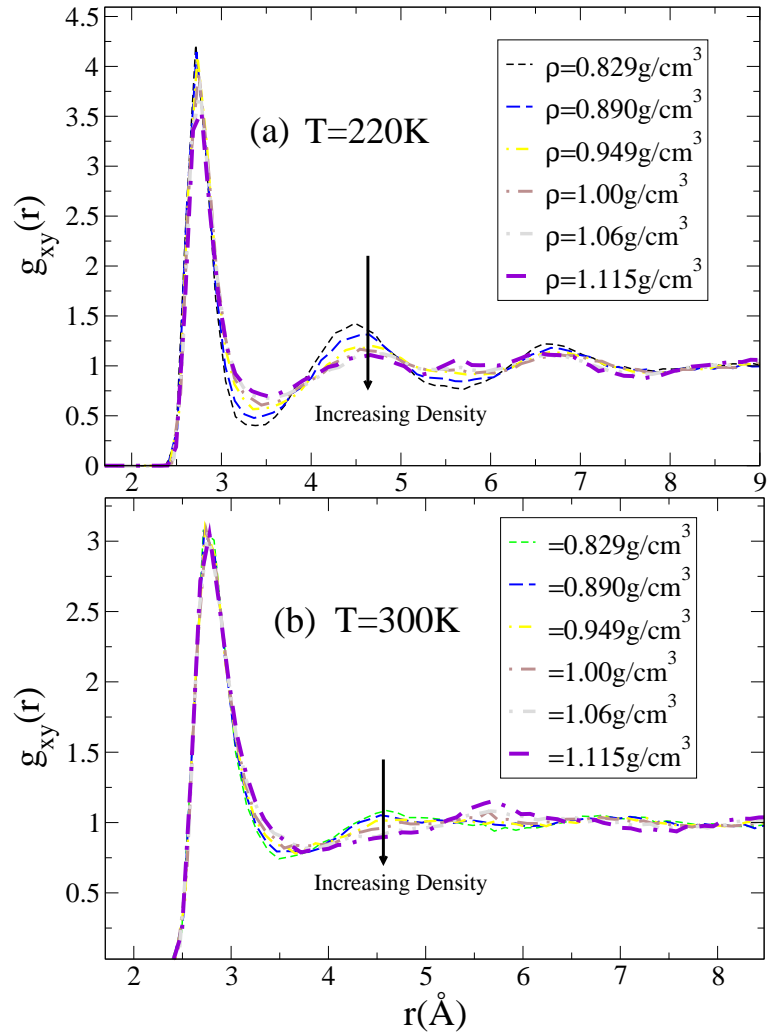


FIG. 5: Lateral oxygen-oxygen pair correlation function  $g_{xy}(r)$  for the case of purely repulsive confinement. Shown are six different densities at two fixed temperatures (a)  $T = 220\text{ K}$  and (b)  $T = 300\text{ K}$ . Note that with increasing density, the second neighbor peak at  $0.45\text{ nm}$  becomes less pronounced and at high temperatures moves to a larger distance.

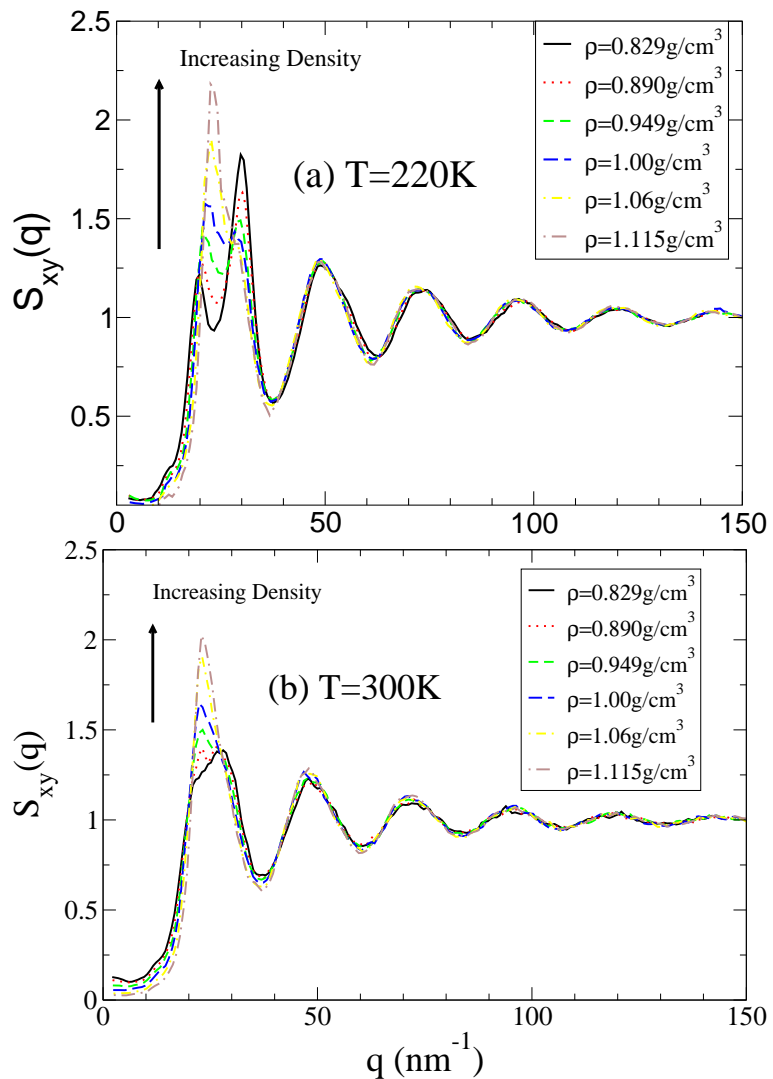


FIG . 6: Lateral structure factor  $S_{xy}(q)$  for the case of repulsive component . Shown are six different densities at two fixed temperatures (a)  $T = 220 \text{ K}$  and (b)  $T = 300 \text{ K}$ . The first peak of  $S_{xy}(q)$  corresponding to the hydrogen-bonds weakens as density is increased and is absent at high densities and high temperatures.

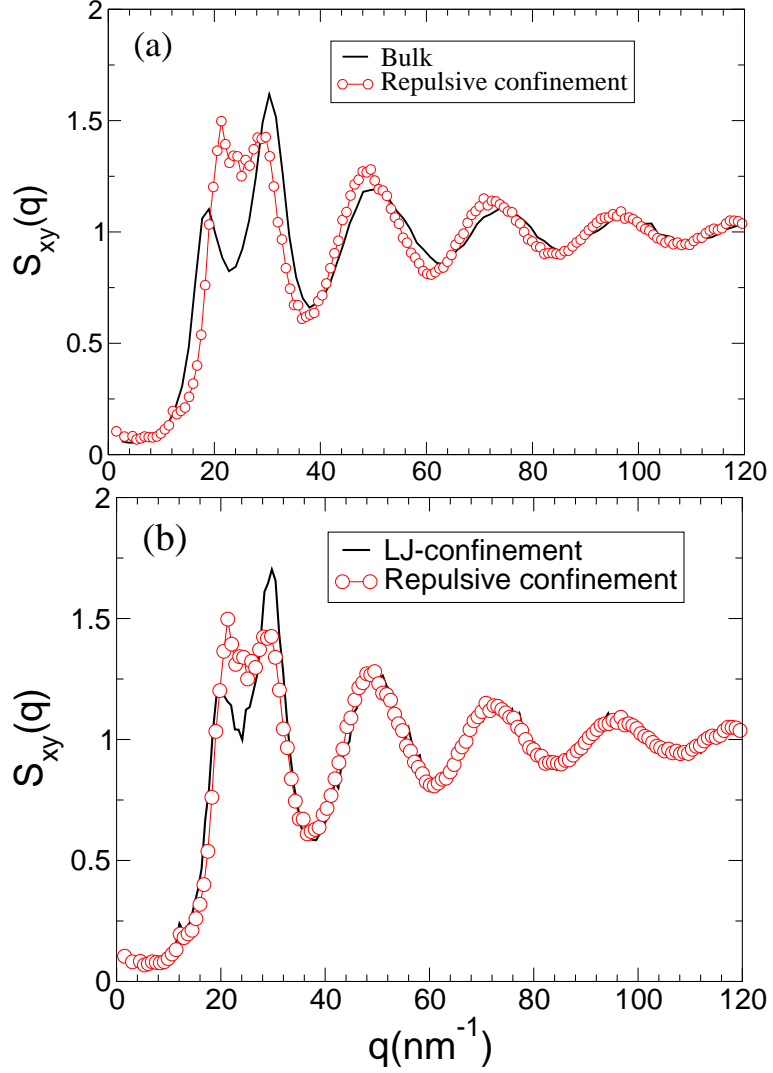


FIG .7: A comparison of the structure factors at  $T = 250\text{K}$  , for the casee of repulsive con nem ent at density  $0.950 \text{ g/cm}^3$  . (a) C om parison ofbulk water water at  $1.00 \text{ g/cm}^3$  w ith repulsive con nem ent. A diminished peak at  $18 \text{ nm}^{-1}$  shows that the local tetrahedral structure is weakened in case of con nem ent. (b) C om parison ofLJ-con nem ent at  $0.950 \text{ g/cm}^3$  w ith repulsive con nem ent. W ater in repulsive con nem ent is less tetrahedral, as the first peak of  $S_{xy}(q)$  is much weaker than the first peak of  $S_{xy}(q)$  for LJ-con nem ent.

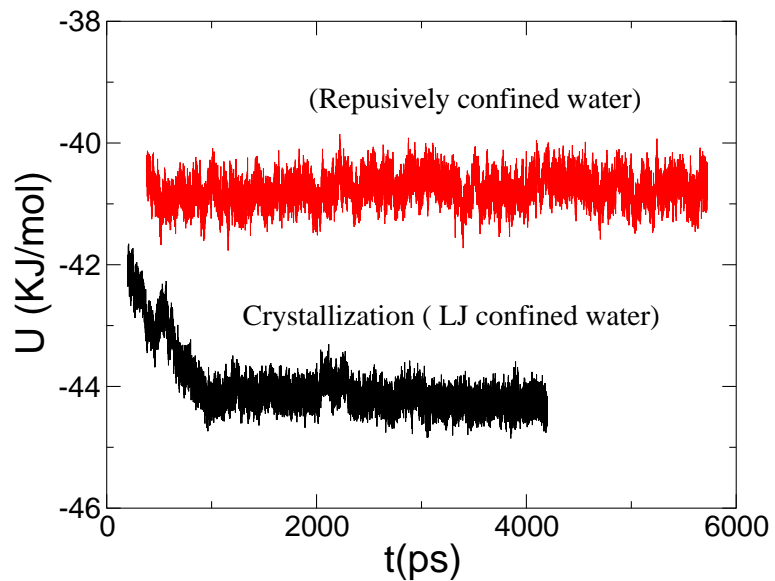


FIG .8: Comparison of the potential energies of purely repulsive confinement, and LJ confinement, both at the same "raw" geometric density  $0.981 \text{ g/cm}^3$  and temperature  $T = 260 \text{ K}$ . The LJ confined system crystallizes, indicated by a sharp drop in the potential energy of the system, while we find no such crystallization in repulsively confined water.

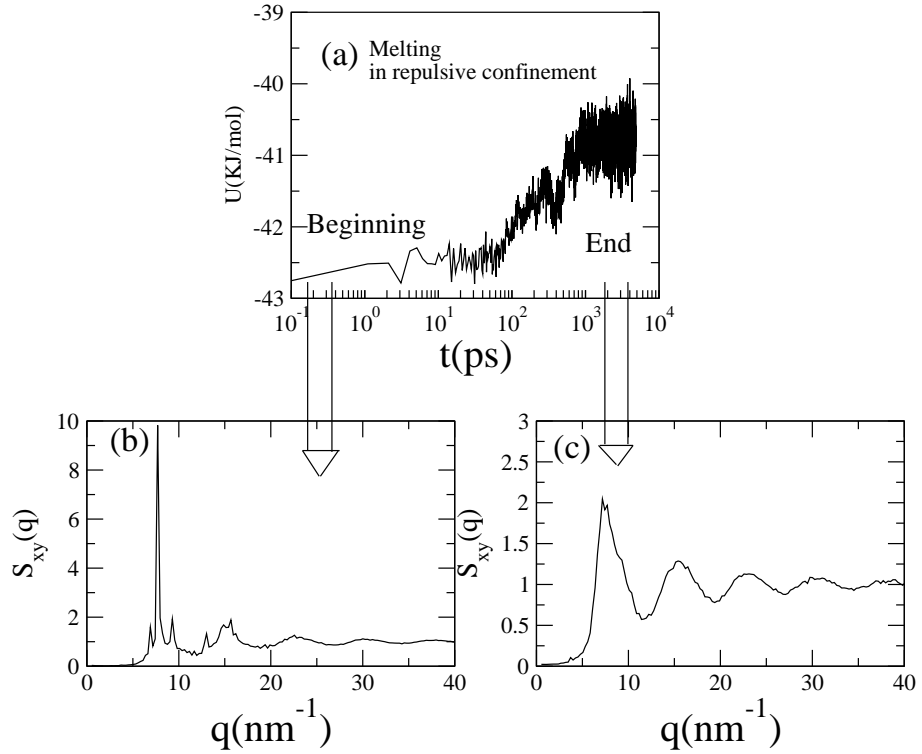


FIG . 9: (a) A plot of potential energy as a function of  $t$ , when the crystal formed in LJ-confinement [12] is kept between the purely repulsive wall. (b) The crystal structure indicated by the sharp Bragg peaks melts, and (c) turns into a liquid indicated by the absence of the Bragg peaks.

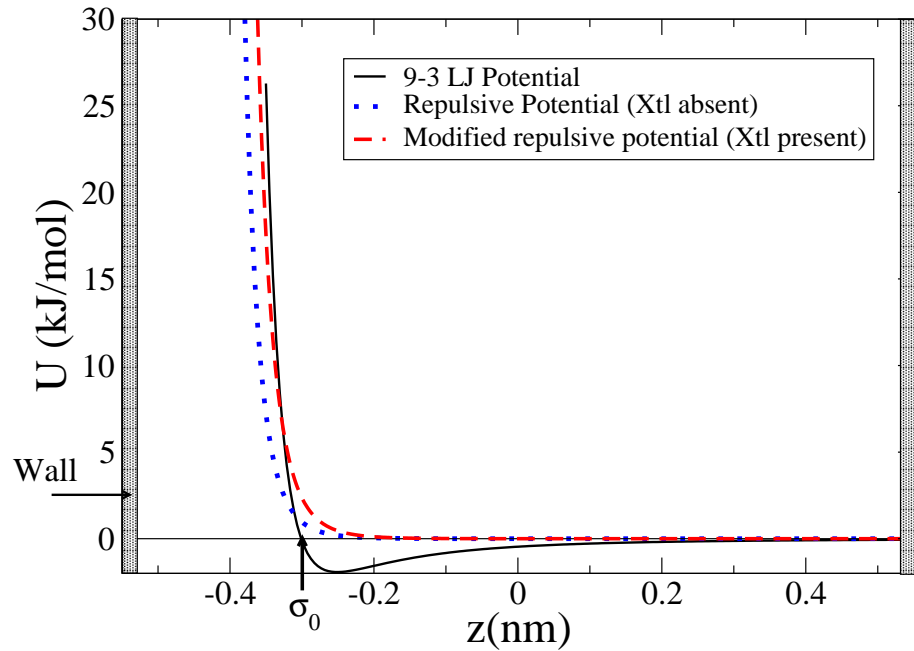


FIG . 10: Water-wall interaction potential, showing LJ and repulsive potentials. LJ potential is shown as a solid black line, repulsive potential is shown as a dotted blue line and the dashed red curve is the modified repulsive potential in order to get the same effective  $L_z$  for purely repulsive component as the effective  $L_z$  in LJ component. When the effective  $L_z$  is same, the liquid in purely repulsive component spontaneously freezes into a trilayer ice (see Fig. 11,12).

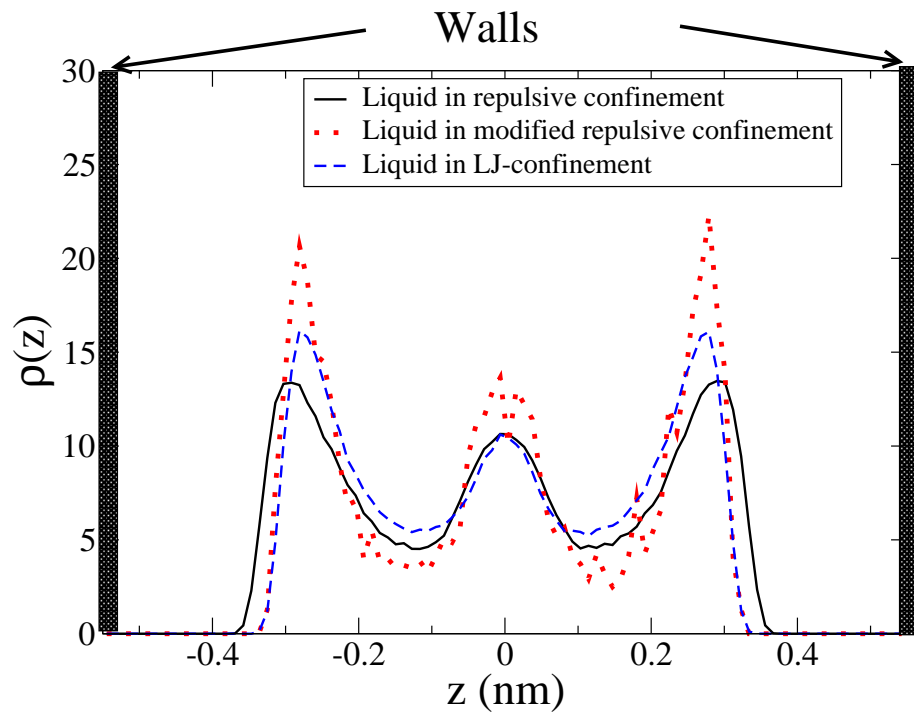


FIG. 11: Density profile  $\rho(z)$  of water along  $z$ -direction for different potentials at the same "raw" geometric density. The repulsive confinement system freezes spontaneously when the parameters of the potential are modified such that the effective  $L_z$  calculated from the  $\rho(z)$  (red dotted line) for the repulsive system is same as that for the LJ-system (blue-dotted line) (see Figs. 10).

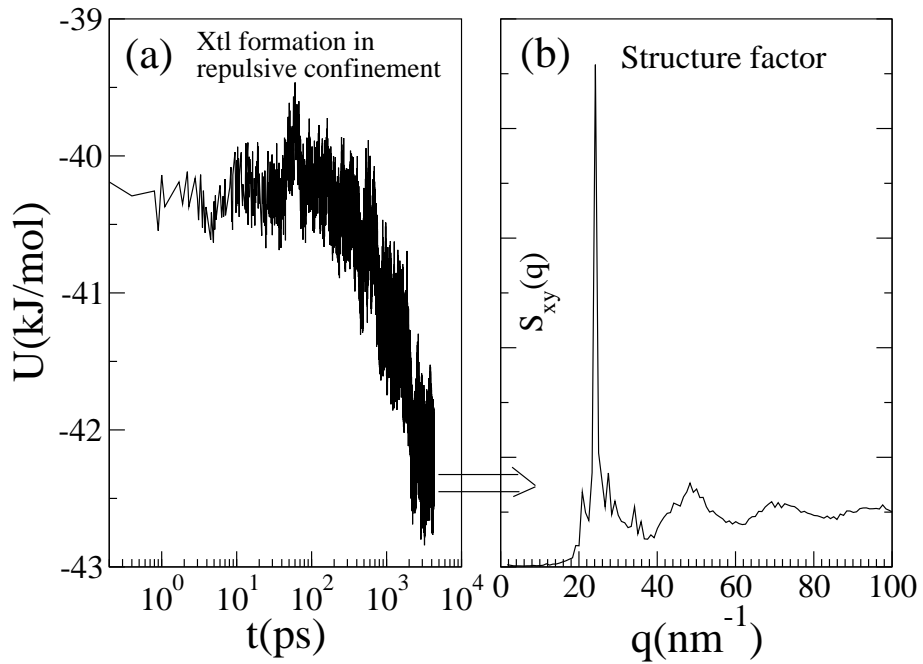


FIG . 12: (a) Potential energy as a function of time  $t$ , for purely repulsive confinement when the effective  $L_z$  is same as the effective  $L_z$  of LJ-confinement at  $T = 260$  K and  $\rho = 0.981$  g/cm $^3$ . The confined water spontaneously freezes, indicated by the drop in potential energy. (b) The structure factor of the ice such formed is resembles the trilayer ice seen in case of LJ confinement [10, 12].